iScience

CellPress
OPEN ACCESS

Article

Patient-derived organoids as personalized avatars and a potential immunotherapy model in cervical cancer

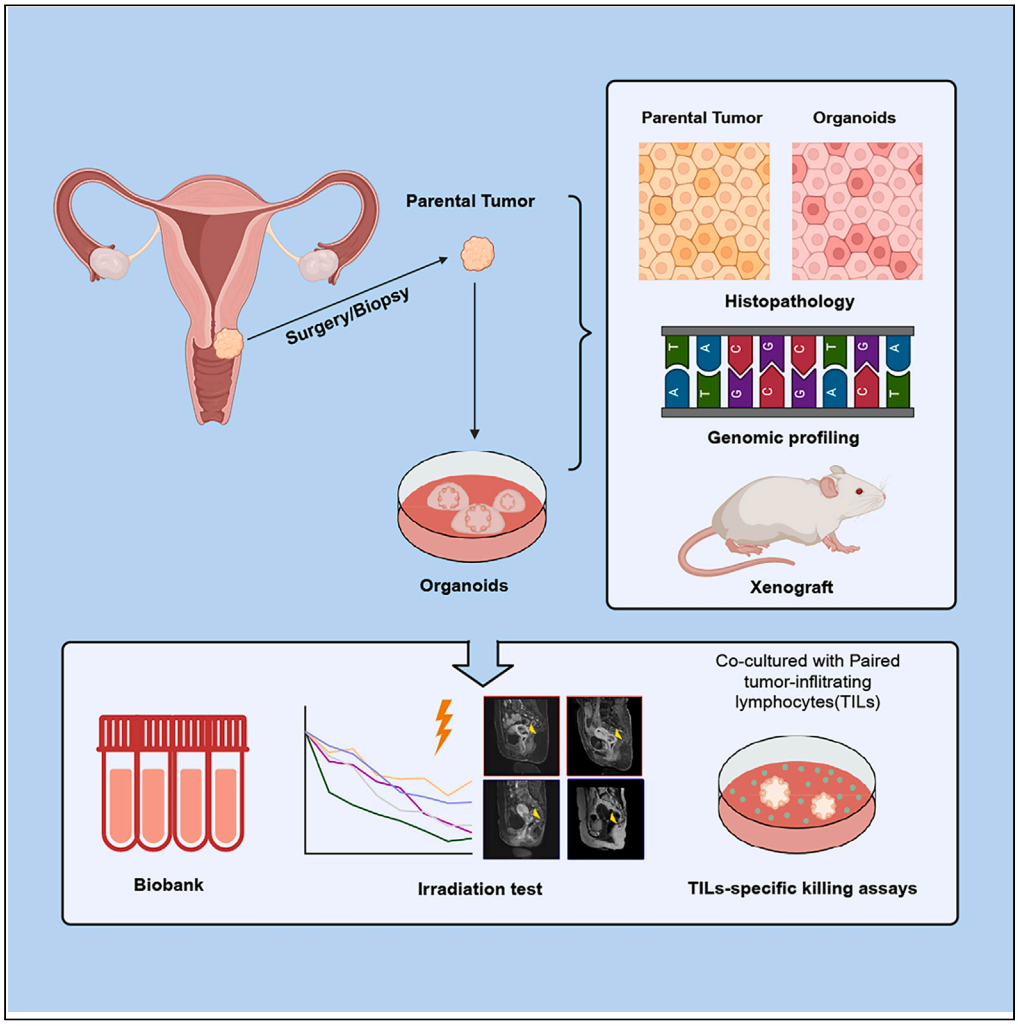

Hua Huang, Yuwen Pan, Jiaming Huang, ..., Chao yun Pan, Junxiu Liu, Shuzhong Yao

liujxiu@mail.sysu.edu.cn (J.L.)
yaoshuzh@mail.sysu.edu.cn (S.Y.)

Highlights

Established a cervical cancer organoids' biobank using an improved culture system

Biobank's utility to capture patients' radiotherapy heterogeneity was demonstrated

Organoid-TILs co-culture system showed potential for studying adoptive T cell therapy

Huang et al., iScience 26, 108198
November 17, 2023
https://doi.org/10.1016/j.isci.2023.108198

iScience

CellPress
OPEN ACCESS

Article

Patient-derived organoids as personalized avatars and a potential immunotherapy model in cervical cancer

Hua Huang,[1,4] Yuwen Pan,[1,4] Jiaming Huang,[1,4] Chunyu Zhang,[1] Yuandong Liao,[1] Qiqiao Du,[1] Shuhang Qin,[1] Yili Chen,[1] Hao Tan,[1] Ming Chen,[1] Manman Xu,[1] Meng Xia,[1] Yunyun Liu,[3] Jie Li,[1] Tianyu Liu,[1] Qiaojian Zou,[1] Yijia Zhou,[1] Li Yuan,[1] Wei Wang,[1] Yanchun Liang,[1] Chao yun Pan,[2] Junxiu Liu,[1,*] and Shuzhong Yao[1,5,*]

SUMMARY

Cervical cancer remains a significant health issue in developing countries. However, finding a preclinical model that accurately reproduces tumor characteristics is challenging. Therefore, we established a patient-derived organoids (PDOs) biobank containing 67 cases of heterogeneous cervical cancer that mimic the histopathological and genomic characteristics of parental tumors. The *in vitro* response of the organoids indicated their ability to capture the radiological heterogeneity of the patients. To model individual responses to adoptive T cell therapy (ACT), we expanded tumor-infiltrating lymphocytes (TILs) *ex vivo* and co-cultured them with paired organoids. The PDOs-TILs co-culture system demonstrates clear responses that correspond to established immunotherapy efficiency markers like the proportion of CTLs. This study supports the potential of the PDOs platform to guide treatment in prospective interventional trials in cervical cancer.

INTRODUCTION

Cervical cancer ranks as the fourth most commonly diagnosed and lethal cancer among women.[1,2] In 2020, there were 604,000 newly confirmed cases of cervical cancer globally, and 342,000 deaths were recorded.[1] In response, the World Health Organization (WHO) has called for the elimination of cervical cancer through three strategies, namely, the popularization of human papillomavirus (HPV) vaccination, promotion of cervical screening, and improvement of treatment and palliative care for aggressive cancer.[3–5] However, long-term observation over several decades is required to evaluate the epidemiological effects of these strategies on cancer prevention. Additionally, the rates of HPV vaccination and cervical screening remain inadequate in middle- and low-income countries,[6,7] contributing to the persistent burden of cervical cancer in developing countries for several decades.[1,8,9]

Treatment options for cervical cancer, including surgical resection, radiotherapy, and chemotherapy, have limitations in their efficacy and can be significantly toxic for recurrent or metastatic patients.[10] In recent years, immunotherapy emerges as a promising approach to treat patients with cervical cancer.[11] However, the efficacy of immunotherapy varies significantly among patients due to the complexity and heterogeneity of solid tumors.[12,13] Therefore, it is necessary to develop preclinical models that can accurately assess the efficacy and mechanisms of these therapies.[12]

Mouse syngeneic tumor models and patient-derived xenografts (PDXs) are commonly used models that include immune components.[14–16] However, while mouse syngeneic tumor models allow for the study of whole-body systemic response to treatment, they cannot fully represent the complex tumor microenvironment in patients.[17–19] PDX, on the other hand, can capture tumor heterogeneity and retain tumor microenvironment composition in immunodeficient mice, but it is not cost-effective or suitable for massive treatment screening.[16,20] As an alternative, patient-derived organoids (PDOs) are *ex vivo* three-dimensional constructs that accurately recapitulate parental tumor characteristics and are suitable for drug screening.[21–24] Therefore, we established a cervical cancer organoid platform and observe its potential for the clinical translation of cell-based immunotherapies.

We established a PDO biobank containing 67 cases of heterogeneous cervical cancer that mimicked the histopathological and genomic features of parental tumors. The response of *ex vivo* organoids demonstrated their ability to capture patient radiation heterogeneity. Cervical cancer organoids also showed different reactions when co-cultured with paired tumor-infiltrating lymphocytes (TILs).

[1]Department of Obstetrics and Gynecology, the First Affiliated Hospital, Sun Yat-sen University, Guangzhou 510080, Guangdong, China
[2]Department of Biochemistry, Zhongshan School of Medicine, Sun Yat-sen University, Guangzhou 510275, China
[3]Sun Yat-Sen Memorial Hospital of Sun Yat-sen University, Guangzhou 510120, China
[4]These authors contributed equally
[5]Lead contact
*Correspondence: liujxiu@mail.sysu.edu.cn (J.L.), yaoshuzh@mail.sysu.edu.cn (S.Y.)
https://doi.org/10.1016/j.isci.2023.108198

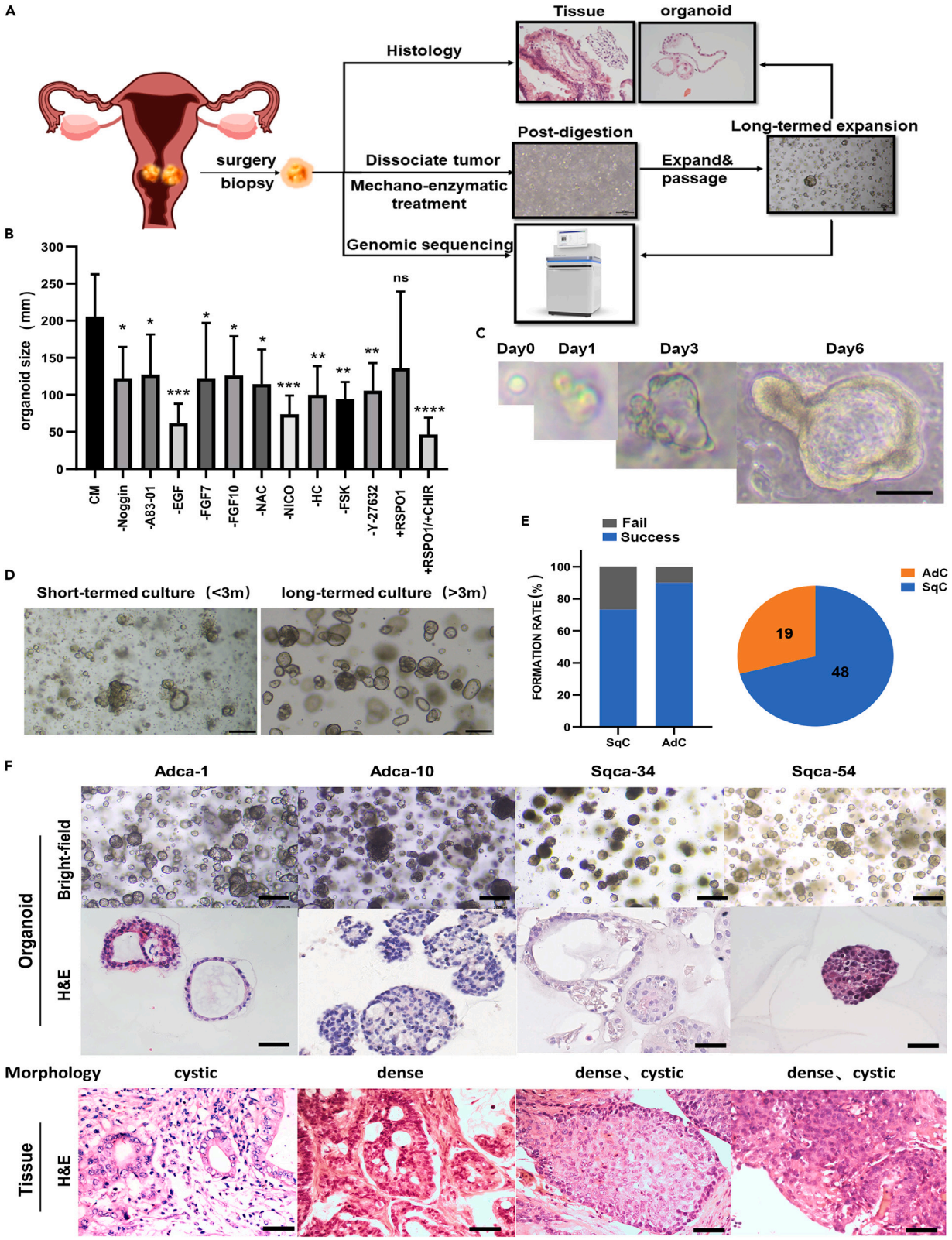
A
Tissue
organoid
Histology
surgery
biopsy
Post-digestion
Long-termed expansion
Dissociate tumor
Mechano-enzymatic treatment
Expand&
passage
Genomic sequencing
B
organoid size (mm)
300
250
200
150
100
50
0
ns
*
**
***
****
CM
-Noggin
-A83-01
-EGF
-FGF7
-FGF10
-NAC
-NICO
-HC
-FSK
-Y-27632
+RSPO1
+RSPO1/+CHIR
C
Day0
Day1
Day3
Day6
D
Short-termed culture (<3m)
long-termed culture (>3m)
E
Fail
Success
FORMATION RATE (%)
100
80
60
40
20
0
SqC
AdC
AdC
SqC
19
48
F
Adca-1
Adca-10
Sqca-34
Sqca-54
Organoid
Bright-field
H&E
Morphology
cystic
dense
dense、cystic
dense、cystic
Tissue
H&E

Figure 1. Generate organoids from different cervical cancer subtypes

A) Workflow diagram of the organoids biobank establishment.

(B) Statistic analysis of different niche factors' effects on the growth of SqC-originated organoids (Compared with complete medium). The size of organoids was recorded after 10 days of culture under the specific medium which means deprivation of certain factors in the complete medium. (Error bars represent the mean ± S.D. of three biologically independent experiments with triplicate repetition).as compared to CM, *p < 0.05, **p < 0.01, ***p < 0.001, ****p < 0.0001, "ns" means "not significant". CM, complete medium; NAC, N-acetyl-L-cysteine; NICO, Nicotinamide; HC, hydrocortisone; FSK, forskolin; Y-27632, ROCK inhibitor; RSPO1, R-spondin 1; CHIR, CHIR 99021. "-" means deprive certain factor in the complete medium; " +" means add a certain factor in the complete medium).

(C) Time course organoid culture of human cervical cancer cell. Represent images of Adca-1. Scale bar, 100 um.

(D) Patient-derived cervical cancer organoids have been dissociated and split every 5–14 days. Representative record of a short-termed culture (<3 m) and a long-termed culture (>3 m). Scale bar, 200 um.

(E) Separated by the pathological type, Left: Organoid formation rates (73.33% for SqC, 90% for AdC); Right: component of cervical cancer organoid biobank (44 cases of SqC,18 cases of AdC).

(F) Organoids resemble the original tumor epithelium morphological structure. Up: bright-field images of organoids, size bar: 200 um; middle & bottom H&E staining of paraffin-embedded organoids and their paired tissue. Scale bar, 50 um.

RESULTS

Establishment of cervical cancer organoids biobank

Ninety-three treatment-naive patients, who provided informed consent, were included in the cervical cancer organoid platform development. (Figure 1A) Small pieces of fresh tumor tissue were collected for organoid culture and histological and genomic analysis after radical surgery or diagnostic biopsy. Dissociated tumor cells or clusters were embedded in Matrigel after mechanical enzymatic digestion using the classic organoid culture method.[25,26] Initially, we used a previously described squamous cell carcinoma (SqC) organoid culture medium,[27] which contained various previously confirmed *in vitro* adult stem cell sustained factors, such as N-acetyl-L-cysteine, nicotinamide, the transforming growth factor β (TGF-β) pathway inhibitor A83-01, the Wnt (Wingless and INT-1) pathway agonist R-spondin 1(RSPO1),[28,29] GSK-3 inhibitors (CHIR 99021), bone morphogenetic protein (BMP) signaling inhibitor noggin, epidermal growth factor (EGF), fibroblast growth factor (FGF) 2, FGF10, and prostaglandin E2.[27,30] Surprisingly, we find that based on this medium, the formation rate of organoids was significantly related to the originated tissue pathological type. The size and expansion capacity of organoids derived from patients with adenocarcinoma (AdC) surpassed those of SqC PDOs (Figure S1A). Although both types originate from metaplasia cells of the cervix transition zone, the factors involved in the switch in the direction of metaplasia carcinogenesis remain unclear. A recent study suggested that opposing Wnt and cyclic AMP (cAMP) signals are pivotal in formation and long-term maintenance of cervical squamous cell organoid.[30] Expecting the presence of the cAMP pathway agonist forskolin (FSK) and the absence of the Wnt pathway agonist RSPO1 might also increase the growth rate of SqC organoids. We set up a complete medium without RSOP1 as a basal medium to identify the essential factors of the SqC organoid culture (Figure S1B). Besides the deprivation of human recombinant EGF severely limiting the development of SqC organoids, the potent activation of the Wnt pathway by adding RSPO1 and CHIR 99021 to the medium caused strong damage to SqC organoid formation (Figure 1B). Following organoid biobank establishment used different medium, including Wnt-excluded medium and Wnt-included medium for SqC and AdC organoid cultures, respectively. Cultured in a suitable niche, examples of cervical cancer organoids formed from a single cell are presented in Figure 1C. Short- and long-term organoids are defined by their ability to expand over 3 months or 10 passages, as described in a previous study.[31] After a long *in vitro* culture period, organoid purity increased (Figure 1D). Six organoids were excluded due to contamination. With an overall success rate of 77%, a total of 67 cervical cancer organoids were established from 87 patients, as well as successfully cryopreserved and resuscitated. Compared to SqC organoids (48/66, 72.7%), there was a slightly higher organoid formation rate in AdC organoids (19/21, 90.5%) (Figure 1E). Among them, the formation rate of long-term organoids had no significant difference between AdC organoids (9/19, 47.4%) and SqC organoids (23/48, 47.9%).

Table 1 shows the fundamental clinical characteristics and data regarding organoid formation of the patients in this biobank. Analyzing the relationship between organoid culture success and original tumor characteristics shows the fundamental clinical characteristics and data regarding organoid formation of the patients in this biobank. Since it includes a broad spectrum of cervical cancers, this dynamic biobank may function as a representative platform for future research on cervical cancer.

PDOs mimic histopathological and genomic features of parental tumors

Cervical cancer PDOs exhibited distinct morphologies *in vitro* (Table 1). Figure 1F up displays the two most common types of tumor morphology, dense and cystic, which often correspond to the pathological types of the parental tumor. AdC-derived organoids were mostly cystic, while SqC-derived organoids were denser. It was also found that H&E staining of Adca-1 organoids revealed a cystic structure, which reproduced the well-differentiated parental tissues with almost normal glandular structures. In contrast, the H&E staining of Adca-10 organoids indicated denser structures related to the moderately differentiated parental tissue pairs, which were distinct from the normal glandular structures. Cellular atypia, including nuclear pleomorphism, high-grade nuclear atypia, and multinucleated giant cells, were present in both organoids and parental tumors.

HPV is known to contribute to oncogenesis in cervical cancers. Genomic DNA was extracted from 10 organoids to compare their integrated HPV types with those of paired tumors. Figure S2 demonstrated that the parental tumors, which had been infected with high-risk types of HPV, were fully retained in the corresponding organoids.

Table 1. Patient clinical data and pair organoids culture state

Patient ID	Age of diagnosis	Tumor FIGO stage	Pathology	Differentiation	First-line treatment	Treatment beside surgery	Sampling event	Organoid label	Organoid Morphology	Culture time (Days)	Organoid culture condition	cryopreservation generation
CC-04	58	Ib1	Squamous cell carcinoma	Moderate	Surgery	Adjuvant[a] Chemotherapy	Surgery	SqCa-1	cystic	42	short-termed culture	P1
CC-05	65	IIIc1	Adenocarcinoma	Moderate	Surgery	Adjuvant Chemotherapy	Biopsy	AdCa-1	dense、cystic	208	long-termed culture	P1-P5
CC-07	42	Ib3	Squamous cell carcinoma	Moderate	Surgery	/	Biopsy	SqCa-2	dense	45	short-termed culture	P2
CC-08	58	IIIb	Squamous cell carcinoma	/	chemoradiation[b]	/	Biopsy	SqCa-3	/	/	Failed	/
CC-09	72	Ib2	Squamous cell carcinoma	/	Surgery	Adjuvant Radiation	Biopsy	SqCa-4	/	/	Failed	/
CC-10	57	IIb	Squamous cell carcinoma	/	chemoradiotion	/	Biopsy	SqCa-5	/	/	Failed	/
CC-12	58	Ib3	Squamous cell carcinoma	Poor-Moderate	Surgery	/	Biopsy	SqCa-6	cystic	32	short-termed culture	P1
CC-13	46	IIa1	Squamous cell carcinoma	Moderate	Surgery	Adjuvant Chemotherapy	Surgery	SqCa-7	dense、cystic	56	short-termed culture	P1-P3
CC-14	43	IIb	Squamous cell carcinoma	/	chemoradiotion	/	Biopsy	SqCa-8	dense	17	short-termed culture	P1
CC-15	49	IIIc1	Squamous cell carcinoma	Poor-Moderate	Surgery	Chemoradiation	Surgery	SqCa-9	/	/	Failed	/
CC-16	55	IIIc1	Squamous cell carcinoma	Moderate	chemoradiation	/	Biopsy	SqCa-10	/	12	short-termed culture	/
CC-17	58	Ivb	Adenocarcinoma	Poor	Surgery	Adjuvant Chemotherapy	Biopsy	AdCa-2	/	/	Failed	/
CC-18	44	IIIc2	Squamous cell carcinoma	Poor-Moderate	chemoradiation	/	Biopsy	SqCa-11	dense、cystic	72	short-termed culture	P1&P3-P4
CC-20	57	Ib3	Squamous cell carcinoma	Poor-Moderate	Surgery	Adjuvant Chemotherapy	Surgery	SqCa-12	dense、cystic	36	short-termed culture	P2
CC-21	41	IIIc1	Squamous cell carcinoma	Poor-Moderate	Surgery	Chemoradiation	Surgery	SqCa-13	dense、cystic	139	long-termed culture	P2-P5
CC-22	66	IIa1	Squamous cell carcinoma	Poor-Moderate	chemoradiation	/	Biopsy	SqCa-14	/	/	Failed	/
CC-23	52	IIIc1	Squamous cell carcinoma	Moderate	Surgery	Chemoradiation	Surgery	SqCa-15	dense	106	long-termed culture	P1&P3&P5

(*Continued on next page*)

Table 1. *Continued*

Patient ID	Age of diagnosis	Tumor FIGO stage	Pathology	Differentiation	First-line treatment	Treatment beside surgery	Sampling event	Organoid label	Organoid Morphology	Culture time (Days)	Organoid culture condition	cryopreservation generation
CC-24	51	Ib2	Squamous cell carcinoma	Poor	Surgery	Adjuvant Chemotherapy	Surgery	SqCa-16	cystic	89	short-termed culture	P2&P3
CC-25	50	Ib1	Adenocarcinoma	/	Surgery	Chemoradiation	Surgery	AdCa-3	dense	167	long-termed culture	P2-P6
CC-26	37	Ib2	Squamous cell carcinoma	Moderate-High	Surgery	Chemoradiation	Surgery	SqCa-17	cystic	65	short-termed culture	P1-P3
CC-27	60	Ib2	Squamous cell carcinoma	Poor	Surgery	/	Surgery	SqCa-18	cystic	65	short-termed culture	P2&P3
CC-28	60	IIb	Squamous cell carcinoma	Moderate	chemoradiation	/	Biopsy	SqCa-19	dense	148	long-termed culture	P1-P5
CC-29	58	Ib3	Squamous cell carcinoma	Moderate	chemoradiation	/	Biopsy	SqCa-20	/	/	Failed	/
CC-30	53	IIIc1	Squamous cell carcinoma	Moderate	Surgery	Chemoradiation	Surgery	SqCa-21	dense、cystic	60	short-termed culture	P1&P2
CC-31	56	IIIc1	Squamous cell carcinoma	Poor-Moderate	Surgery	Adjuvant Chemotherapy	Biopsy	SqCa-22	dense	107	long-termed culture	P2-P5
CC-32	30	Ib2	Adenocarcinoma	Moderate	Surgery	Adjuvant Chemotherapy	Surgery	AdCa-4	cystic	126	long-termed culture	P1-P5
CC-33	46	IIIc1	Squamous cell carcinoma	Poor	Surgery	Adjuvant Chemotherapy	Biopsy	SqCa-23	cystic	72	short-termed culture	P2&P4
CC-34	32	Ib2	Adenocarcinoma	Moderate-High	Surgery	/	Surgery	AdCa-5	cystic	72	short-termed culture	P2-P4
CC-35	65	Ib2	Squamous cell carcinoma	Moderate-High	Surgery	Adjuvant Chemotherapy	Biopsy	SqCa-24	cystic	77	short-termed culture	P1-P4
CC-36	53	IIb	Adenocarcinoma	/	Surgery	Adjuvant Chemotherapy	Biopsy	AdCa-6	cystic	36	short-termed culture	P1&P2
CC-37	55	IIb	Squamous cell carcinoma	Poor	Surgery	Adjuvant Chemotherapy	Biopsy	SqCa-25	dense、cystic	79	short-termed culture	P1-P3
CC-38	50	IIIc1	Squamous cell carcinoma	/	Surgery	Adjuvant Chemotherapy	Biopsy	SqCa-26	dense	87	short-termed culture	P1-P5
CC-39	52	Ib2	Squamous cell carcinoma	Poor-Moderate	Surgery	Adjuvant Chemotherapy	Biopsy	SqCa-27	dense	86	short-termed culture	P2-P5
CC-40	56	IIIc1	Squamous cell carcinoma	Poor-Moderate	Surgery	Chemoradiation	Surgery	SqCa-28	dense	106	long-termed culture	P1-P5

(*Continued on next page*)

Table 1. *Continued*

Patient ID	Age of diagnosis	Tumor FIGO stage	Pathology	Differentiation	First-line treatment	Treatment beside surgery	Sampling event	Organoid label	Organoid Morphology	Culture time (Days)	Organoid culture condition	cryopreservation generation
CC-41	38	IIb	Adenocarcinoma	/	Surgery	Neoadjuvant[c] chemotherapy	Biopsy	AdCa-7	cystic	84	short-termed culture	P1&P3&P4
CC-42	51	Ib3	Squamous cell carcinoma	Moderate-High	Surgery	/	Surgery	SqCa-29	dense	56	short-termed culture	P1-P3
CC-43	58	Ib3	Squamous cell carcinoma	Moderate	Surgery	Adjuvant Chemotherapy	Surgery	SqCa-30	/	/	Failed	/
CC-44	52	IIIc1	Adenocarcinoma	/	Surgery	Adjuvant Chemotherapy	Surgery	AdCa-8	dense、cystic	42	short-termed culture	P1&P2
CC-45	62	Ib1	Squamous cell carcinoma	Poor	Surgery	/	Surgery	SqCa-31	/	/	Failed	/
CC-46	41	Ib2	Squamous cell carcinoma	Poor	Surgery	Adjuvant Chemotherapy	Surgery	SqCa-32	dense、cystic	85	short-termed culture	P2-P4
CC-47	43	IIIc1	Adenocarcinoma	/	Surgery	Adjuvant Chemotherapy	Surgery	AdCa-9	cystic	183	long-termed culture	P1-P5
CC-48	49	Ib2	Adenocarcinoma	Moderate	Surgery	Adjuvant Chemotherapy	Surgery	AdCa-10	dense	114	long-termed culture	P2-P5
CC-49	39	IIIc1	Adenocarcinoma	Poor	Surgery	Adjuvant Chemotherapy	Biopsy	AdCa-11	cystic	231	long-termed culture	P1-P5
CC-50	53	Ib1	Squamous cell carcinoma	/	Surgery	/	Surgery	SqCa-33	dense、cystic	99	long-termed culture	P2&P4&P5
CC-51	57	IIIc1	Adenocarcinoma	/	Surgery	Adjuvant Chemotherapy	Biopsy	AdCa-12	/	/	Failed	/
CC-52	51	Ib1	Squamous cell carcinoma	Poor	Surgery	/	Surgery	SqCa-34	dense	97	long-termed culture	P2-P4
CC-53	65	IIIc2	Squamous cell carcinoma	Poor-Moderate	Surgery	Adjuvant Chemotherapy	Surgery	SqCa-35	/	/	Failed	/
CC-54	50	IIIc1	Adenocarcinoma	Well	Surgery	/	Biopsy	AdCa-13	cystic	35	short-termed culture	P2&P3
CC-55	49	IIIc2	Adenocarcinoma	/	Surgery	/	Biopsy	AdCa-14	cystic	80	short-termed culture	P1-P4
CC-56	46	IIIC1p	Squamous cell carcinoma	Moderate	Surgery	Adjuvant Chemotherapy	Surgery	SqCa-36	dense	61	short-termed culture	P2&P3
CC-57	63	IIA1	Squamous cell carcinoma	Moderate-High	Surgery	Adjuvant Chemotherapy	Surgery	SqCa-37	dense	62	short-termed culture	P1-P3

(*Continued on next page*)

Table 1. *Continued*

Patient ID	Age of diagnosis	Tumor FIGO stage	Pathology	Differentiation	First-line treatment	Treatment beside surgery	Sampling event	Organoid label	Organoid Morphology	Culture time (Days)	Organoid culture condition	cryopreservation generation
CC-58	31	IB2	Squamous cell carcinoma	Poor-Moderate	Surgery	/	Surgery	SqCa-38	dense、cystic	112	long-termed culture	P2-P5
CC-59	46	IIIC1p	Squamous cell carcinoma	Moderate	Surgery	Chemoradiation	Surgery	SqCa-39	dense	192	long-termed culture	P1-P5
CC-60	63	IIA1	Squamous cell carcinoma	Poor	chemoradiation	/	Biopsy	SqCa-40	dense、cystic	143	long-termed culture	P1-P5
CC-61	62	IB2	Squamous cell carcinoma	Moderate	Surgery	Chemoradiation	Surgery	SqCa-41	dense	89	short-termed culture	P2&P3&P5
CC-62	63	IIA1	Squamous cell carcinoma	Poor-Moderate	Surgery	Chemoradiation	Surgery	SqCa-42	dense、cystic	184	long-termed culture	P1-P4
CC-63	47	IIIC1p	Squamous cell carcinoma	Poor	Surgery	Chemoradiation	Surgery	SqCa-43	dense	54	short-termed culture	P1&P2
CC-64	49	IIIC1p	Squamous cell carcinoma	Poor	chemoradiation	/	Biopsy	SqCa-44	dense	175	long-termed culture	P1-P5
CC-65	64	IB2	Squamous cell carcinoma	Poor	Surgery	Adjuvant Chemotherapy	Surgery	SqCa-45	dense	171	long-termed culture	P2-P5
CC-66	39	IIIC2p	Squamous cell carcinoma	Poor	Surgery	Adjuvant Chemotherapy	Surgery	SqCa-46	dense	106	long-termed culture	P2-P5
CC-67	28	IIIC1r	Squamous cell carcinoma	Poor	Surgery	Neoadjuvant chemotherapy	Biopsy	SqCa-47	/	/	Failed	/
CC-68	46	IB3	Squamous cell carcinoma	Poor-Moderate	Surgery	Chemoradiation	Surgery	SqCa-48	dense	101	long-termed culture	P2-P4
CC-69	35	IIIC2P	Squamous cell carcinoma	Moderate	Surgery	Adjuvant Chemotherapy	Surgery	SqCa-49	dense	144	long-termed culture	P1-P5
CC-70	63	IIA1	Squamous cell carcinoma	Poor	Surgery	Chemoradiation	Surgery	SqCa-50	/	/	Failed	/
CC-71	47	IB2	Squamous cell carcinoma	Poor	Surgery	/	Surgery	SqCa-51	dense	76	short-termed culture	P2&P3
CC-72	55	IVB	Adenocarcinoma	/	Surgery	/	Surgery	AdCa-15	cystic	39	short-termed culture	P2
CC-73	56	IIA1	Adenocarcinoma	Poor	Surgery	Adjuvant Chemotherapy	Surgery	AdCa-16	dense、cystic	153	long-termed culture	P1-P5
CC-74	32	IB1	Adenosquamous carcinoma	Moderate	Surgery	Adjuvant Chemotherapy	Surgery	AdCa-17	dense、cystic	144	long-termed culture	P1-P5

(*Continued on next page*)

Table 1. *Continued*

Patient ID	Age of diagnosis	Tumor FIGO stage	Pathology	Differentiation	First-line treatment	Treatment beside surgery	Sampling event	Organoid label	Organoid Morphology	Culture time (Days)	Organoid culture condition	cryopreservation generation
CC-75	28	IB2	Squamous cell carcinoma	Poor-Moderate	Surgery	Adjuvant Chemotherapy	Surgery	SqCa-52	dense	18	short-termed culture	/
CC-76	40	IIA1	Squamous cell carcinoma	Moderate	Surgery	Chemoradiation	Surgery	SqCa-53	dense	106	long-termed culture	P2-P4
CC-77	63	IB2	Squamous cell carcinoma	Poor	Surgery	Chemoradiation	Surgery	SqCa-54	dense、cystic	118	long-termed culture	P1-P5
CC-78	48	IB2	Adenosquamous carcinoma	Poor	Surgery	/	Surgery	SqCa-55	dense	106	long-termed culture	P1-P5
CC-79	59	IB2	Adenocarcinoma	Moderate	Surgery	Chemoradiation	Surgery	AdCa-18	cystic	89	short-termed culture	P2&P3&P5
CC-80	59	IB2	Squamous cell carcinoma	Moderate	Surgery	/	Surgery	SqCa-56	dense	86	long-termed culture	P1-P3
CC-81	61	IB2	Adenocarcinoma	/	Surgery	/	Surgery	AdCa-19	cystic	80	short-termed culture	P1&P2
CC-82	54	IB3	Squamous cell carcinoma	Poor-Moderate	Surgery	Chemoradiation	Surgery	SqCa-57	dense	96	long-termed culture	P2-P5
CC-83	32	IB2	Adenocarcinoma	/	Surgery	/	Surgery	AdCa-20	cystic	135	long-termed culture	P2-P5
CC-84	73	IB2	Squamous cell carcinoma	Moderate	Surgery	/	Surgery	SqCa-58	dense	45	short-termed culture	P2&P3
CC-85	56	IIIC1p	Squamous cell carcinoma	Poor	Surgery	Chemoradiation	Surgery	SqCa-59	dense、cystic	56	short-termed culture	P1-P3
CC-86	57	IB3	Squamous cell carcinoma	Moderate	Surgery	Chemoradiation	Surgery	SqCa-60	dense	78	short-termed culture	P1-P4
CC-87	55	IIIC1p	Squamous cell carcinoma	Poor-Moderate	Surgery	Chemoradiation	Biopsy	SqCa-61	dense、cystic	123	long-termed culture	P1-P5
CC-88	66	IIA1	Squamous cell carcinoma	Moderate	Surgery	/	Surgery	SqCa-62	dense	95	long-termed culture	P2-P5
CC-89	58	IIIC1p	Squamous cell carcinoma	Poor-Moderate	Surgery	Chemoradiation	Surgery	SqCa-63	/	/	Failed	/
CC-90	56	IIA1	Squamous cell carcinoma	Moderate	Surgery	/	Surgery	SqCa-64	dense、cystic	78	on-going	P2-P4

(*Continued on next page*)

Table 1. *Continued*

Patient ID	Age of diagnosis	Tumor FIGO stage	Pathology	Differentiation	First-line treatment	Treatment beside surgery	Sampling event	Organoid label	Organoid Morphology	Culture time (Days)	Organoid culture condition	cryopreservation generation
CC-91	53	IB2	Adenocarcinoma	/	Surgery	/	Surgery	AdCa-21	cystic	75	on-going	P1-P3
CC-92	40	IIA1	Squamous cell carcinoma	Poor	Surgery	/	Surgery	SqCa-65	/	/	Failed	/
CC-93	50	IIA1	Squamous cell carcinoma	Poor-Moderate	Surgery	/	Surgery	SqCa-66	dense	69	on-going	P1-P3

[a]"Adjuvant Chemotherapy" or "Adjuvant radiotherapy" mean chemotherapy or radiotherapy treatment following tumor resection.
[b]"chemoradiation" means radiation with chemosensitization.
[c]"Neoadjuvant chemotherapy" means treatment before tumor resection.

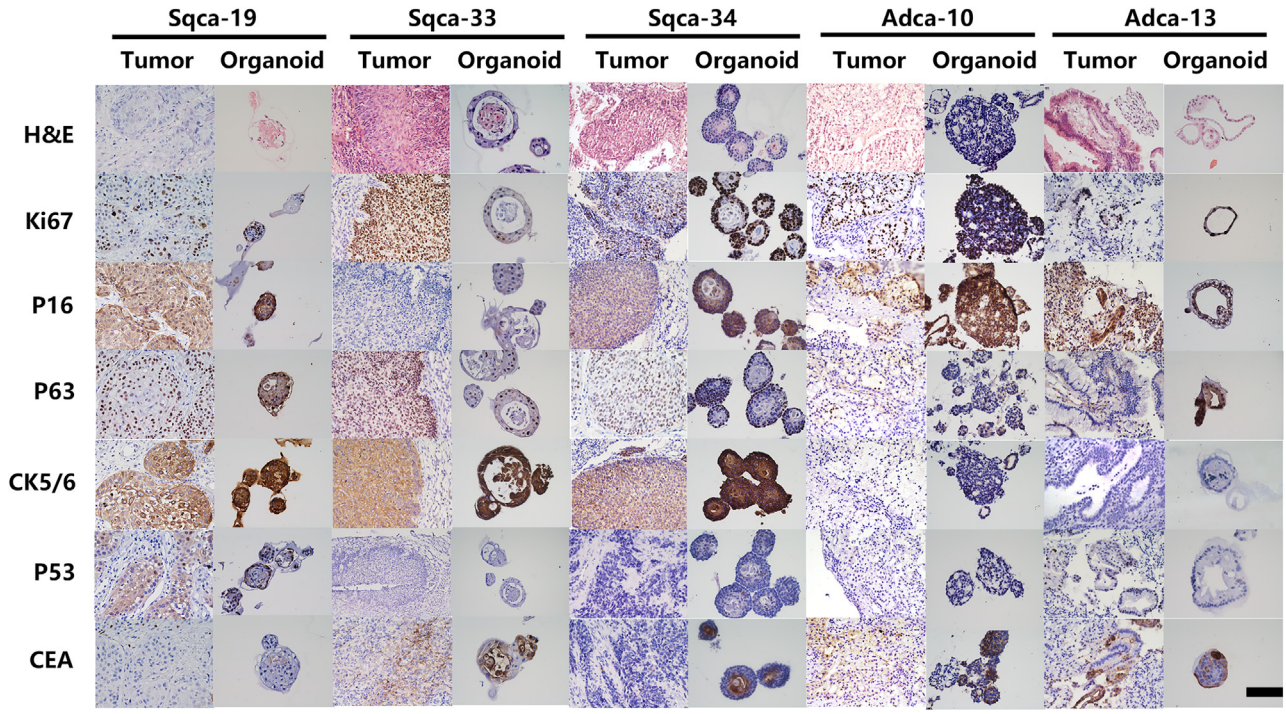

Figure 2. PDOs mimic the Histological characteristics of the parental tumors

H&E-stained and IHC-stained images of representative SqC organoids, AdC organoids, and their respective original cervical cancer tissues. Tissue and organoids were stained for H&E, Ki67, P16, P63, CK5/6, P53, and CEA. (Scale bar, 100 μm).

As has been noted in other studies, after long-term *in vitro* culture, tumor tissue-derived organoids only contain malignant epithelial tumor cells, excluding immune cells, vessels, or connective tissue.[25–27] As shown in Figure 2, immunohistochemical staining was used to compare the histopathological features of the long-term cultured organoids and paired parental tumors. Organoids retained the epithelial tumor cell portions of their parental tumors. Organoids with fast growth, such as Sqca-34 and Adca-10, demonstrated a strong expression of Ki67, a marker of proliferation. The high-risk HPV-infected indicator, P16, was positive in both HPV+ parental tumors and paired organoids, such as Adca-10 derived from a patient with HPV 18+, Sqca-19, and Sqca-34 derived from patients with HPV 16+. Moreover, the high immunoreactivity for CK5/6 observed in the SqC organoids indicates their characteristic features of squamous cells. In contrast, the AdC organoids did not show any CK5/6 immunoreactivity. Positive carcinoembryonic antigen (CEA) expression has been demonstrated in cervical cancer, especially concerning AdC and keratinizing SqC. AdC organoids show positive expression of CEA, similar to their parental tumor, while CEA expression may depend on cell differentiation in SqC organoids.

Whole-exome sequencing (WES) was performed on a subset of organoid lines to quantify whether the genomic landscape of the cervical cancer organoids was faithfully retained from the corresponding tumors. Using ABSOLUTE algorithm analysis revealed similar DNA copy number variation patterns throughout the whole genome between organoids and their paired tumors when the parental tumor was of high purity (Figure 3A). To further determine the genetic correlation between organoids and their driven parental tumors, somatic mutations were analyzed (Figures 3B, S3A, and S3B). Both cervical cancer tissues and paired organoids exhibited significant distribution of C > T mutations among six types of somatic single-nucleotide variants (SNVs) (Figure S3A). This finding concurs with the previously described mutational spectrum for cervical cancer.[31] Significantly mutated genes of cervical cancer, such as *PIK3CA*, *EP300*, *FBXW7*, *PTEN*, *ARID1A*, and *TTN* were identified in our organoid biobank. These genes were identified to be mutated in cervical cancer patients' genomic characterizations, similar to previous studies of large cohorts (Figures 3B; Table S1).[31–34] Overall, our organoid biobank recapitulated genetic alterations in cervical cancer, confirming the representativeness of parental tumors.

Ex vivo organoids response captures patients' radiotherapy heterogeneity

Besides surgery, radiation is another first-line treatment for cervical cancer. We exposed 14 cervical cancer organoids to radiation *ex vivo*. We observed a significant difference in organoid response among patients by monitoring changes in organoid size, which is indicative of organoid survival. For example, Sqca-34 exhibited higher radiosensitivity than Sqca-19 (Figure 4A). The CellTiter-Glo 3D viability assay was used to evaluate the organoid activity in different radiotherapy dose groups. Displayed as dose-response curves and area under the curve (AUC) calculations, the spectrum of dose responses indicated *ex vivo* organoid radiosensitivity heterogeneity (Figures 4B and 4C). We then asked whether the different sensitivities exhibited in the *ex vivo* organoid model correlated with clinical outcomes. For advanced cervical cancer

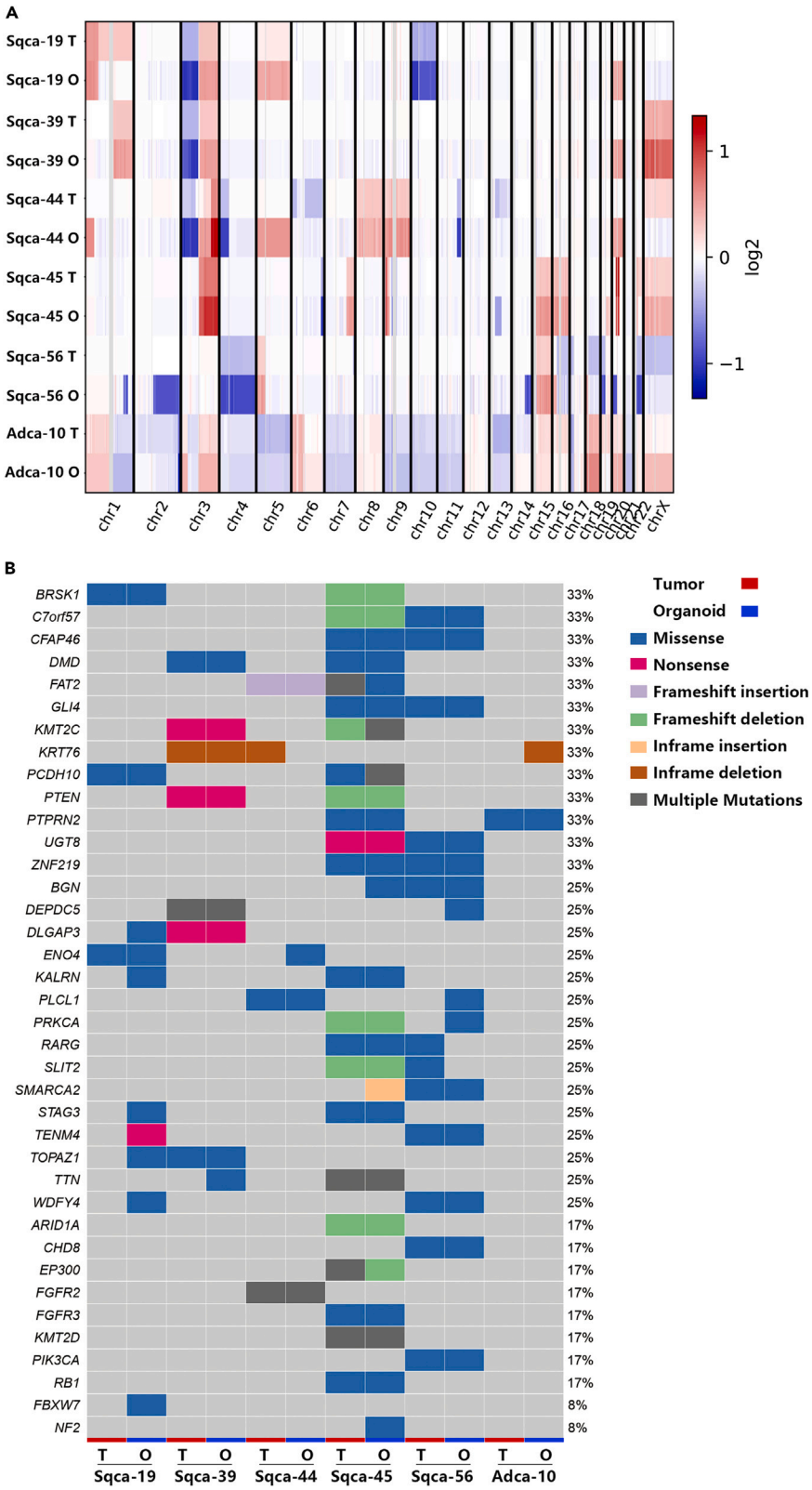
A
Sqca-19 T
Sqca-19 O
Sqca-39 T
Sqca-39 O
Sqca-44 T
Sqca-44 O
Sqca-45 T
Sqca-45 O
Sqca-56 T
Sqca-56 O
Adca-10 T
Adca-10 O
chr1
chr2
chr3
chr4
chr5
chr6
chr7
chr8
chr9
chr10
chr11
chr12
chr13
chr14
chr15
chr16
chr17
chr18
chr19
chr20
chr21
chr22
chrX
1
0
−1
log2
B
BRSK1
C7orf57
CFAP46
DMD
FAT2
GLI4
KMT2C
KRT76
PCDH10
PTEN
PTPRN2
UGT8
ZNF219
BGN
DEPDC5
DLGAP3
ENO4
KALRN
PLCL1
PRKCA
RARG
SLIT2
SMARCA2
STAG3
TENM4
TOPAZ1
TTN
WDFY4
ARID1A
CHD8
EP300
FGFR2
FGFR3
KMT2D
PIK3CA
RB1
FBXW7
NF2
33%
33%
33%
33%
33%
33%
33%
33%
33%
33%
33%
33%
33%
25%
25%
25%
25%
25%
25%
25%
25%
25%
25%
25%
25%
25%
25%
25%
17%
17%
17%
17%
17%
17%
17%
17%
8%
8%
T O T O T O T O T O T O
Sqca-19 Sqca-39 Sqca-44 Sqca-45 Sqca-56 Adca-10
Tumor
Organoid
Missense
Nonsense
Frameshift insertion
Frameshift deletion
Inframe insertion
Inframe deletion
Multiple Mutations

Figure 3. PDOs retained genomic feature of the parental tumors

(A) Heatmap presented the copy number variation (CNV) of different chromosomes. Logarithmic the value of CNV (visualized as color-coded). Colors range from blue (CNV decreased) to red (CNV increased).

(B) Somatic mutations and insertion/deletion in PDOs and parental tumor tissues.

patients, the standard treatment is radiotherapy combined with platinum-based chemotherapy.[35] We investigated how cervical cancer organoids could serve as a preclinical platform for studying the effects of radiation with chemosensitization. To match the patients' treatment responses, studies were conducted on two tumor organoids from patients with advanced cervical cancer who underwent radiation with chemosensitization. Sqca-19 and Sqca-44 organoids were irradiated in combination with cisplatin at a concentration of approximately (20% inhibitory concentration) IC20 (5 uM) (Figure S4). Under the same experimental conditions, for Sqca-44 PDOs, cisplatin has demonstrated a sensitizing effect on radiation on Sqca-44, whereas Sqca-19 PDOs showed no effect (Figure 4D). The response of these two patients to clinical chemoradiation therapy was assessed using magnetic resonance imaging (MRI) three months after treatment (Figure 4E). According to the RECIST(Response Evaluation Criteria in Solid Tumours) evaluation, patient Sqca-44 exhibited a complete response (CR) to chemoradiation, while patient Sqca-19 showed a partial response (PR). Besides imaging findings, the variation trend of serum squamous cell carcinoma antigen (SCC) differed between these two patients. The serum SCC level of patient Sqca-19 increased from 4.3 μg/L (before treatment) to 6.39 μg/L (three months after treatment). In contrast, the serum SCC level of patient Sqca-44 decreased from 1.6 μg/L to 0.9 μg/L after treatment. The comparison between clinical outcomes and *ex vivo* organoid treatment responses indicates the potential of *ex vivo* organoids to correspond to clinical treatment responses. Taken together, these data demonstrate that organoids derived from cervical cancer display varied sensitivities to radiation treatment. Furthermore, the data provide more evidence supporting the application of the tumor organoid model in preclinical studies of cervical cancer.

Organoid platform: A potential model for adoptive cellular immunotherapy research

Similar to other adult tissue-derived organoids, our cervical cancer organoids only contained malignant epithelial tumor cells after long-term *in vitro* culturing.[25,26,28] To investigate the potency of PDOs in adoptive cellular immunotherapy, we paired seven organoids and their TILs for *in vitro* TIL-specific killing assays. TILs were extracted and expanded according to the classical protocol.[37] After a 3-day co-culture (E:T = 10:1), organoid apoptosis and tumor-specific TILs activation were measured (Figure S5A). To directly observe organoids' apoptosis situation and locate TILs after co-culture, we used live cell dye to label organoids (Cell trace Far Red), TILs (Cell trace Yellow), and caspase3/7 probe traced apoptosis cells (Figures 5A and S5B). Compared to the control groups, unblocked tumor-specific TILs induced a significant presence of caspase3/7-positive cells in Sqca-45, Sqca-56, Sqca-62, and Adca-21, as demonstrated by the results (Figure 5B). There was a significant decrease in the anti-apoptotic protein Bcl2 in the Sqca-56 co-culture group (Figure 5C, bottom). The co-culture group with Sqca-39-, Sqca-61-, and Sqca-64-specific TILs did not significantly increase the proportion of caspase3/7-positive cells (Figure 5B) or induce a significant decrease in Bcl2 (Figure 5C, up). The significantly higher apoptotic cell level in the co-cultured group, as compared to the major histocompatibility complex (MHC)-blocked group, showed that Sqca-45, Sqca-56, Sqca-62, and Adca-21 organoids were responsive to *in vitro* paired TILs killing assay. In contrast Sqca-39, Sqca-61, and Sqca-64 were classified as the non-responsive group when co-cultured with paired TILs. These results indicated that the killing efficiency of different tumor-specific TILs varied *in vitro*. Additionally, the levels of interferon (IFN) γ secretion and the frequency of T cell effector markers CD107a and CD137 were summarized after co-culture (Figures 5D, S5C, and S5D). The production of the antitumor cytokine IFNγ was markedly enhanced when T cells of Sqca-45, Sqca-56, Sqca-62, and Adca-21 were effected in the co-culture system (Figure 5D). The number of T cells expressing the CD137 activation marker increased (Figures S5C and S5E) when TILs from Sqca-45 were exposed to paired tumor organoids. This phenomenon corresponds to the high level of killing capacity previously reported. To figure out the factors that affect the effectiveness of *in vitro* adoptive cellular immunotherapy, immune cell typing and tumor mutation load were examined using flow cytometry and WES (Figures 5E and S3D). When comparing responsive group and non-responsive group, the TILs of the non-responsive group severely lacked cytotoxic T lymphocytes (CTLs), directly resulting in weak killing efficacy (Figure 5E). This was also reflected in the TILs surrounding the organoids of the responsive group (Figure 5C). Regrettably, it is not feasible to accurately predict clinical immunotherapy prognosis. However, the above results illustrate the potential of the PDOs platform for *in vitro* prediction of adoptive cellular immunotherapy efficacy.

PDOs retain tumorigenicity and radiosensitivity in immune deficiency xenograft

Tumorigenicity is an important characteristic of tumor-derived organoids. We subcutaneously transplanted four separate lines of cervical cancer organoid (Sqca-19, Sqca-42, Adca-1, and Adca-10) into immunodeficient mice (n = 4 in each group) to test whether the PDOs retained their tumorigenic potential. Injections were performed on two flanks of each animal. After 5 weeks, all the organoid lines produced macroscopically visible tumors under the subcutaneous tissue (Figure 6A). All except one of the four organoid lines (Sqca-19, Sqca-42, and Adca-1) exhibited complete xenograft success after eight weeks of injection (Figure 6B). H&E and immunohistochemical staining of the excised xenograft tumors was performed to identify their origin (Figures 6C and S6A). When PDO regrew and infiltrated *in vivo*, PDO xenografts (PDOXs) recapitulated the histological architecture of the parental tumor (Figure 6C). For example, tumor nests that exhibit the characteristics of stratification and keratinization are driven by SqC. PDOX originated from AdC contains disordered glands or glandular structures with irregular sizes and shapes. Strong diffuse P16 staining revealed that three PDOXs (Sqca-19, Sqca-42, and Adca-10) were infected with high-risk HPV (Figure S6A, middle). PDOs' tumorigenicity was well maintained as all four PDOX cases showed positive Ki67 expression (Figure S6A, bottom).

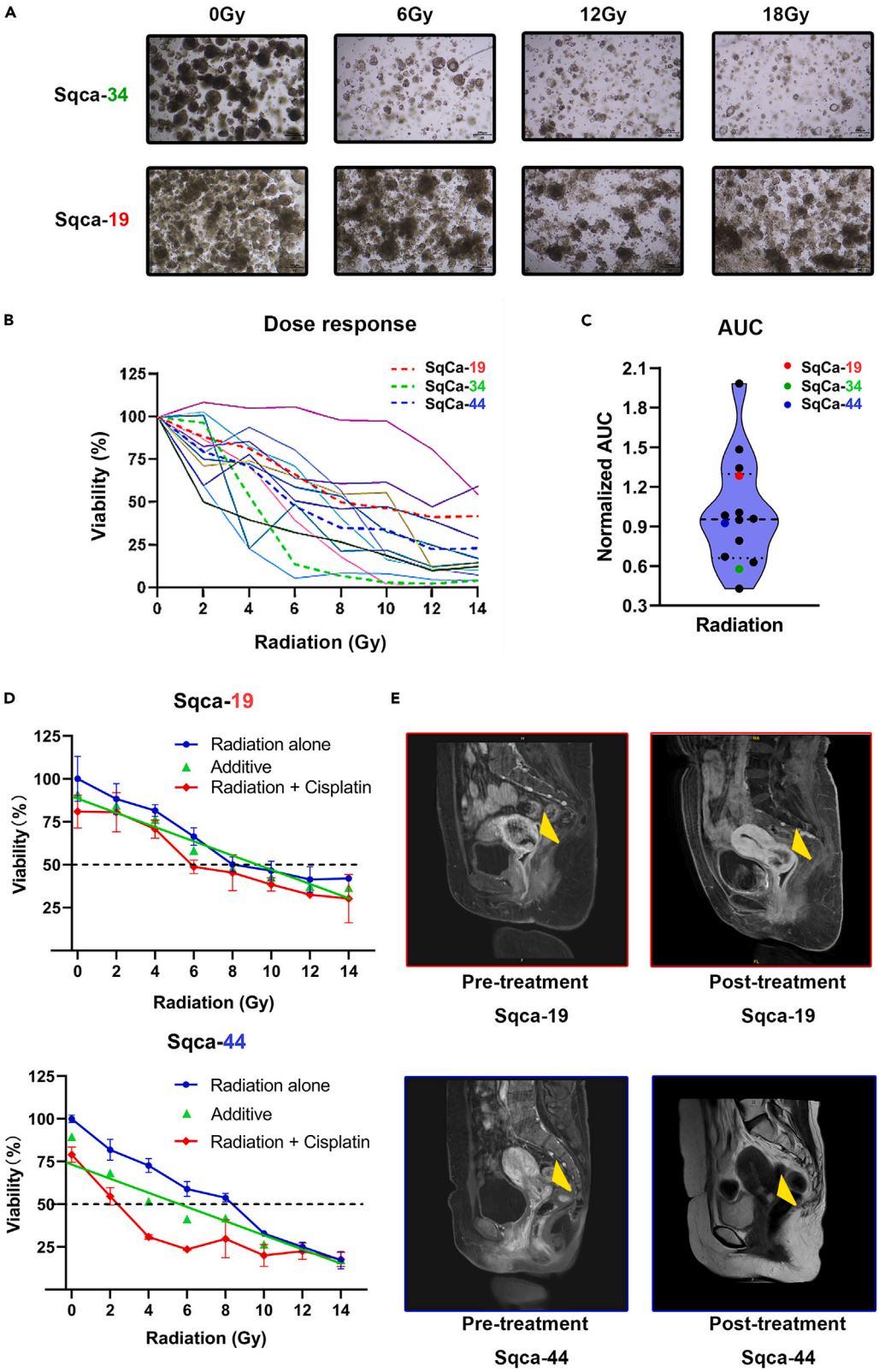
A
0Gy
6Gy
12Gy
18Gy
Sqca-34
Sqca-19
B
Dose response
SqCa-19
SqCa-34
SqCa-44
Viability (%)
Radiation (Gy)
C
AUC
SqCa-19
SqCa-34
SqCa-44
Normalized AUC
Radiation
D
Sqca-19
Radiation alone
Additive
Radiation + Cisplatin
Viability (%)
Radiation (Gy)
Sqca-44
Radiation alone
Additive
Radiation + Cisplatin
Viability (%)
Radiation (Gy)
E
Pre-treatment
Sqca-19
Post-treatment
Sqca-19
Pre-treatment
Sqca-44
Post-treatment
Sqca-44

Figure 4. *Ex vivo* organoids responses to radiation and clinically relevant CRT

(A) Representative bright-field images of organoids dose-response to radiation treatment (organoids on day 6 after radiation in two selected cases).

(B and C) *Ex vivo* radiosensitivity of 14 cervical cancer organoids (each sample contained 2/3 independent experiments) is displayed in B. dose-response curve with the corresponding AUC calculation as shown in C. Colored data dots indicate those organoids referenced in A, D, and E.

(D) Representative dose-response curves of the Sqca-19 & Sqca-44 treated with radiation alone and radiation combined with 5 μM cisplatin. Great synergy was exhibited by the combinational treatment of radiation and cisplatin on Sqca-44. The dose-response curve of combinational treatment was significantly lower than the additive effect curve; it was classified as effective chemosensitization.[36]

(E) The Sqca-19 & Sqca-44 patients' clinical cervical cancer was viewed by magnetic resonance imaging (MRI) according to routine clinical care pre-treatment (yellow arrow, tumor) and after CRT (yellow arrow, tumor). Referring to the RECIST standard, patient Sqca-44 was complete response (CR) to CRT, while patient Sqca-19 was partial response (PR).

In vivo radiotherapy was conducted using the Sqca-42 & Sqca-19 PDOX. One week following the radiotherapy, compared with Sqca-19 PDOX, Sqca-42 PDOX revealed an immediate growth restriction (Figures S6B and S6C). Continuous observation over a month showed that *in vivo* radiotherapy resulted in significant tumor suppressions in the Sqca-42 PDOX model. According to histopathological analysis, radiation reduced the size of Sqca-42 PDOX tumor and caused considerable tumor necrosis (Figures S6C and S6D, Left). No limitation in tumor growth was observed in the Sqca-19 PDOX model due to radiotherapy (refer Figures S6C and S6D, Right). The above results are consistent with the organoids' radiosensitivity observed in *ex vivo* organoid radiosensitivity tests (see Figures 4B and 4C).

DISCUSSION

Recently, the organoid technique has become widely popular due to its wide range of applications in disease modeling and compound screening.[25,26,30–33] However, there has been no established research on cervical cancer organoids until last year, considering their low incidence in high-income countries and high susceptibility to contamination.[34] To tackle this problem, an enhanced cervical cancer organoid culture system was developed to improve the culture protocol and enable long-term expansion. Including 67 samples, we successfully established a large cervical cancer organoid biobank. H&E staining and immunohistochemistry (IHC) revealed that basic histopathological characteristics and markers that indicated keratinization or HPV infection were well conserved between organoids and parental tumors (Figure 2; Table S2). Using WES and qPCR, the mutation profiles of established organoid lines were found to be similar to those of their originated tumor tissues. *In vivo* xenografts retained PDOs tumorigenicity. And PDOX recapitulates the histological features of the parental tumor. This organoid platform is directly derived from patients and represents the heterogeneity of cervical cancer patients.

Several tissues from the patient were procured from biopsy samples. Our study showed the feasibility of deriving organoid models from biopsy samples, with a success rate of 72.4% (21/29). This suggests that organoid models can be derived from cervical biopsy samples, which are less harmful and can be obtained at various stages such as diagnosis, before or after treatment, or at the time of recurrence. Sensitivity tests conducted *in vitro* and *in vivo* can facilitate precise treatment within 1–3 months of establishment, regardless of whether standard or experimental therapeutics are used. To investigate organoids' potential for clinical translation, and the correlation between the sensitivity of *ex vivo* tumor organoids and clinical outcomes, 2 patients who underwent radiotherapy with chemosensitization were enrolled in this assay. Prior to treatment, organoids were created and exposed to a combination of radiation and cisplatin. *Ex vivo* experiments demonstrated that cisplatin functions as a radiosensitizer in Sqca-44, and this is associated with the patient's complete response to chemoradiation (Figures 4D and 4E).

Another attractive feature of this study was the establishment of an organoid-TIL co-culture system. We analyzed the *ex vivo* CTLs killing effects of CTLs on organoids and T cells. However, the *ex vivo* killing assay results varied among the patients, despite similar experimental conditions (Figure 5). Previous studies suggest a correlation between *TTN* mutation and high tumor mutation burden (TMB). These studies also indicate that *TTN* mutation can potentially predict a positive response to immune checkpoint blockade treatment in immunotherapy-sensitive solid tumors like cervical cancer.[32] Our study showed that Sq-45, which exhibited a significantly stronger *ex vivo* treatment response, also retained the *TTN* mutation (Figure 3B). These data support the hypothesis that *TTN* mutation might be relevant to the response to adoptive T cell therapy (ACT). This might hint at *TNN*'s potential on being a cervical cancer ACT effect predictor. However, this model mimics only the interaction between tumor cells and TILs and neglects other components in the tumor microenvironment, as well as the participation of the peripheral lymphatic system. This weakness makes co-culture models more suitable for *ex vivo* generation and screening of tumor-specific CTLs.[38] Exploring the tumor-derived organoid reserved tumor microenvironment might be more suitable for immunotherapy response tests.[35] In summary, we have established a large cervical cancer organoid biobank and provided a platform for *ex vivo* treatment response studies. Such research might help identify therapeutic biomarkers that distinguish responders from non-responders, potentially save patients from toxic side effects, and increase the cost of useless treatment.

Limitations of the study

In this study, regrettably, most of our enrolled patients underwent surgical treatment, unable to conduct prospective validation in a larger cohort. To fully investigate organoids' potential for predicting clinical treatment responses, a comprehensive study involving multiple patients and tumor organoids would be needed.

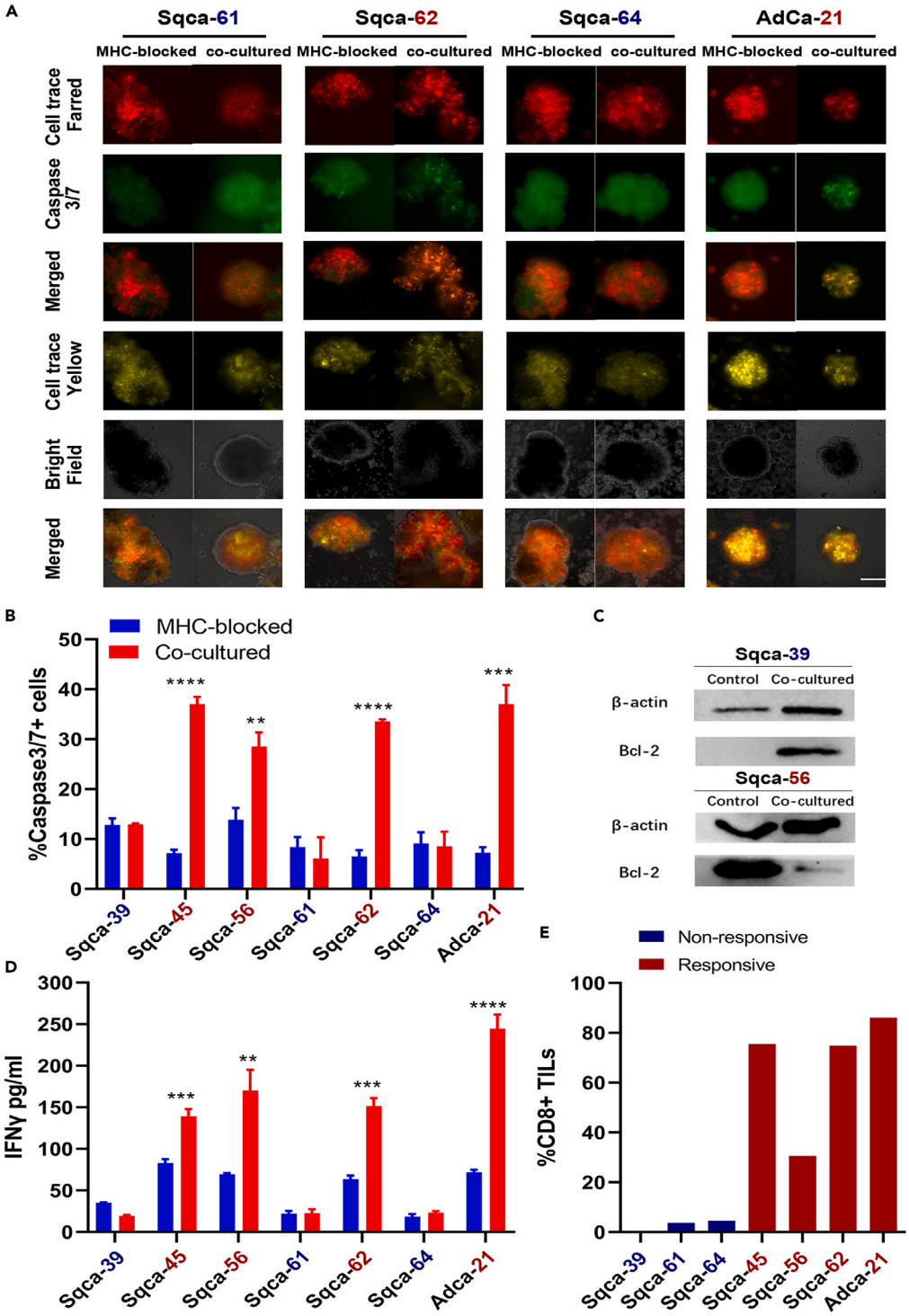

Figure 5. Paired TILs killing assay in cervical cancer organoid models

(A) Represent fluorescent images showed the control group and co-cultured group of Sqca-61, Sqca-62, Sqca-64, &Adca-21. Cell Trace FarRed labeled organoids (red), and caspase 3/7 probe labeled apoptotic cells(green), Cell Trace Yellow labeled co-cultured TILs (yellow). Scale bar, 50μm.

(B) Summary of the caspase3/7+ apoptotic cells frequency from each group by using flow cytometry detecting FITC signal caspase 3/7 probe).

(C)Bcl2 protein expression in Sqca-39 & Sqca-45 validated by western blot.

(D) IFNγ level (pg/ml) in each co-cultured system was detected using an ELISA kit.

(E) The frequency of $CD8^+$ TILs of each case in two group was detected by flow cytometry.

(Error bars represent the mean ± S.D. of three biologically independent experiments with triplicate repetition, *p < 0.05, **p < 0.01, ***p < 0.001).

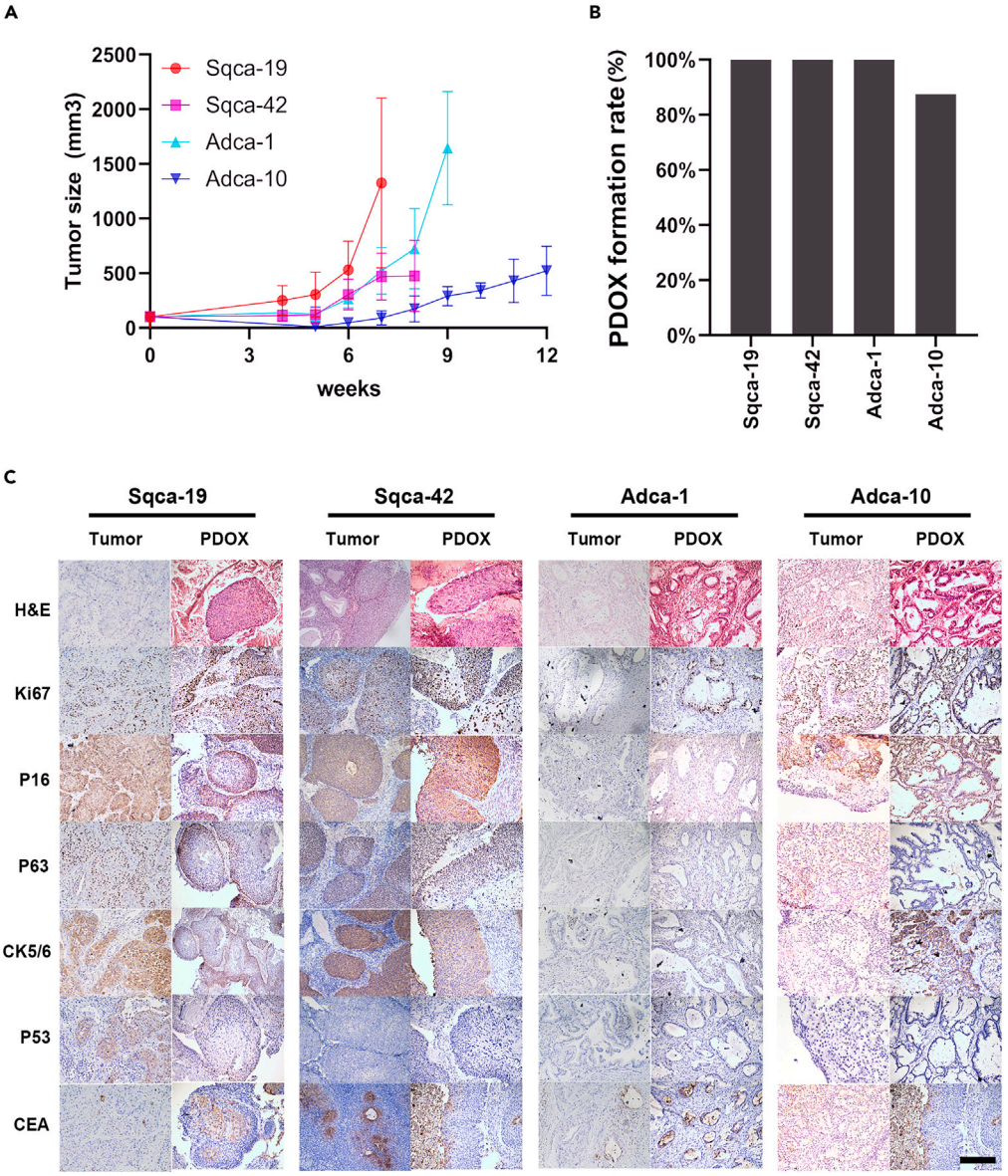

Figure 6. PDOXs recapitulated the features of the parental tumors

(A) Tumor growth curves (n = 7 or 8) indicate different growth rates of each PDOX.

(B) Xenograft formation rate (n = 7 or 8).

(C) Representative images of H&E staining and IHC staining of the paraffin-embedded tumor. Black scale bar, 100 μm.

STAR★METHODS

Detailed methods are provided in the online version of this paper and include the following:

- KEY RESOURCES TABLE
- RESOURCE AVAILABILITY
  - Lead contact
  - Materials availability
  - Data and code availability
- EXPERIMENTAL MODEL AND STUDY PARTICIPANT DETAILS
- METHOD DETAILS
  - Tissue procession

- TILs *ex vivo* expansion
- H&E staining and IHC
- DNA extraction and HPV detection
- Genomic analysis and TMB
- *Ex vivo* organoids radiation and chemosensitization treatment
- Organoids killing assay
- Flow cytometry
- Organoid xenograft and In vivo PDOX radiotherapy

- QUANTIFICATION AND STATISTICAL ANALYSIS

SUPPLEMENTAL INFORMATION

Supplemental information can be found online at https://doi.org/10.1016/j.isci.2023.108198.

ACKNOWLEDGMENTS

We thank the Pathology Department of the First Affiliated Hospital of Sun Yat-sen University for supporting the histological identification of organoids. We acknowledge Professor Wenyi Gu for TILs ex vivo expansion technology. This work was supported by the National Key R&D Program of China (2022YFC2704200& 2022YFC2704201 to SZY), National Natural Science Foundation of China (81874102& 82072874 to SZY, 81502226& 81872128 to JXL), Science and Technology Plan of Guangdong Province (2023A0505050102 to SZY), Guangzhou Science and Technology Program (202002020043 to SZY), and Sun Yat-sen University Clinical Research Foundation of 5010 Project (2017006 to SZY).

AUTHOR CONTRIBUTIONS

Conception: H.H., Y.P., J.H., J.L., and S.Y.; Methodology & Investigation: H.H., Y.P., J.H., C.Z., Y.Liu., and Q.D.; Resources: H.H., Y.P., S.Q., Y.C., H.T., M.C., M.Xu., M.Xia, J.Li., and T.L.; Formal Analysis & Visualization: H.H., J.H., Y.L., Q.Z., Y.Z., and L.Y.; Writing—Original Draft: H.H., Y.P., and J.H.; Writing—Review & Editing: H.H., Y.P., Y.Liang., W.W., and C.y.P.; Supervision: Y.Liang., W.W., C.y.P., J.Liu., and S.Y.; Project Administration: H.H., J.Liu., and S.Y.; Funding Acquisition: J.Liu. and S.Y.

DECLARATION OF INTERESTS

The authors declare no competing interests.

Received: April 25, 2023
Revised: May 5, 2023
Accepted: October 10, 2023
Published: October 12, 2023

REFERENCES

1. Sung, H., Ferlay, J., Siegel, R.L., Laversanne, M., Soerjomataram, I., Jemal, A., and Bray, F. (2021). Global Cancer Statistics 2020: GLOBOCAN Estimates of Incidence and Mortality Worldwide for 36 Cancers in 185 Countries. CA. Cancer J. Clin. *71*, 209–249.
2. Zhang, X., Zeng, Q., Cai, W., and Ruan, W. (2021). Trends of cervical cancer at global, regional, and national level: data from the Global Burden of Disease study 2019. BMC Publ. Health *21*, 894.
3. Alfaro, K., Maza, M., Cremer, M., Masch, R., and Soler, M. (2021). Removing global barriers to cervical cancer prevention and moving towards elimination. Nat. Rev. Cancer *21*, 607–608.
4. Astbury, K., and Turner, M.J. (2009). Human papillomavirus vaccination in the prevention of cervical neoplasia. Int. J. Gynecol. Cancer *19*, 1610–1613.
5. Das, M. (2021). WHO launches strategy to accelerate elimination of cervical cancer. Lancet Oncol. *22*, 20–21.
6. Doherty, M., Buchy, P., Standaert, B., Giaquinto, C., and Prado-Cohrs, D. (2016). Vaccine impact: Benefits for human health. Vaccine *34*, 6707–6714.
7. Spayne, J., and Hesketh, T. (2021). Estimate of global human papillomavirus vaccination coverage: analysis of country-level indicators. BMJ Open *11*, e052016.
8. Canfell, K., Kim, J.J., Brisson, M., Keane, A., Simms, K.T., Caruana, M., Burger, E.A., Martin, D., Nguyen, D.T.N., Bénard, É., et al. (2020). Mortality impact of achieving WHO cervical cancer elimination targets: a comparative modelling analysis in 78 low-income and lower-middle-income countries. Lancet *395*, 591–603.
9. Knaul, F.M., Rodriguez, N.M., Arreola-Ornelas, H., and Olson, J.R. (2019). Cervical cancer: lessons learned from neglected tropical diseases. Lancet. Glob. Health *7*, e299–e300.
10. Chung, H.C., Ros, W., Delord, J.P., Perets, R., Italiano, A., Shapira-Frommer, R., Manzuk, L., Piha-Paul, S.A., Xu, L., Zeigenfuss, S., et al. (2019). Efficacy and Safety of Pembrolizumab in Previously Treated Advanced Cervical Cancer: Results From the Phase II KEYNOTE-158 Study. J. Clin. Oncol. *37*, 1470–1478.
11. Hu, Z., and Ma, D. (2018 Oct). The precision prevention and therapy of HPV-related cervical cancer: new concepts and clinical implications. Cancer Med. *7*, 5217–5236.
12. Hegde, P.S., and Chen, D.S. (2020). Top 10 Challenges in Cancer Immunotherapy. Immunity *52*, 17–35.
13. Ando, Y., Mariano, C., and Shen, K. (2021). Engineered in vitro tumor models for cell-based immunotherapy. Acta Biomater. *132*, 345–359.
14. Siolas, D., and Hannon, G.J. (2013). Patient-derived tumor xenografts: transforming clinical samples into mouse models. Cancer Res. *73*, 5315–5319.
15. Tentler, J.J., Tan, A.C., Weekes, C.D., Jimeno, A., Leong, S., Pitts, T.M., Arcaroli, J.J., Messersmith, W.A., and Eckhardt, S.G. (2012). Patient-derived tumour xenografts as models for oncology drug development. Nat. Rev. Clin. Oncol. *9*, 338–350.
16. Byrne, A.T., Alférez, D.G., Amant, F., Annibali, D., Arribas, J., Biankin, A.V., Bruna, A., Budinská, E., Caldas, C., Chang, D.K., et al. (2017). Interrogating open issues in cancer precision medicine with patient-derived xenografts. Nat. Rev. Cancer *17*, 254–268.
17. Dranoff, G. (2011). Experimental mouse tumour models: what can be learnt about

human cancer immunology? Nat. Rev. Immunol. *12*, 61–66.
18. Gould, S.E., Junttila, M.R., and de Sauvage, F.J. (2015). Translational value of mouse models in oncology drug development. Nat. Med. *21*, 431–439.
19. Decker, W.K., da Silva, R.F., Sanabria, M.H., Angelo, L.S., Guimarães, F., Burt, B.M., Kheradmand, F., and Paust, S. (2017). Cancer Immunotherapy: Historical Perspective of a Clinical Revolution and Emerging Preclinical Animal Models. Front. Immunol. *8*, 829.
20. Cassidy, J.W., Caldas, C., and Bruna, A. (2015). Maintaining Tumor Heterogeneity in Patient-Derived Tumor Xenografts. Cancer Res. *75*, 2963–2968.
21. Drost, J., and Clevers, H. (2018). Organoids in cancer research. Nat. Rev. Cancer *18*, 407–418.
22. Kim, M., Mun, H., Sung, C.O., Cho, E.J., Jeon, H.J., Chun, S.M., Jung, D.J., Shin, T.H., Jeong, G.S., Kim, D.K., et al. (2019). Patient-derived lung cancer organoids as in vitro cancer models for therapeutic screening. Nat. Commun. *10*, 3991.
23. Seppälä, T.T., Zimmerman, J.W., Sereni, E., Plenker, D., Suri, R., Rozich, N., Blair, A., Thomas, D.L., 2nd, Teinor, J., Javed, A., et al. (2020). Patient-derived Organoid Pharmacotyping is a Clinically Tractable Strategy for Precision Medicine in Pancreatic Cancer. Ann. Surg. *272*, 427–435.
24. Al Shihabi, A., Davarifar, A., Nguyen, H.T.L., Tavanaie, N., Nelson, S.D., Yanagawa, J., Federman, N., Bernthal, N., Hornicek, F., and Soragni, A. (2022). Personalized chordoma organoids for drug discovery studies. Sci. Adv. *8*, eabl3674.
25. Shi, R., Radulovich, N., Ng, C., Liu, N., Notsuda, H., Cabanero, M., Martins-Filho, S.N., Raghavan, V., Li, Q., Mer, A.S., et al. (2020). Organoid Cultures as Preclinical Models of Non-Small Cell Lung Cancer. Clin. Cancer Res. *26*, 1162–1174.
26. Kopper, O., de Witte, C.J., Lõhmussaar, K., Valle-Inclan, J.E., Hami, N., Kester, L., Balgobind, A.V., Korving, J., Proost, N., Begthel, H., et al. (2019). An organoid platform for ovarian cancer captures intra- and interpatient heterogeneity. Nat. Med. *25*, 838–849.
27. Driehuis, E., Kolders, S., Spelier, S., Lõhmussaar, K., Willems, S.M., Devriese, L.A., de Bree, R., de Ruiter, E.J., Korving, J., Begthel, H., et al. (2019). Oral Mucosal Organoids as a Potential Platform for Personalized Cancer Therapy. Cancer Discov. *9*, 852–871.
28. Sato, T., Stange, D.E., Ferrante, M., Vries, R.G.J., Van Es, J.H., Van den Brink, S., Van Houdt, W.J., Pronk, A., Van Gorp, J., Siersema, P.D., and Clevers, H. (2011). Long-term expansion of epithelial organoids from human colon, adenoma, adenocarcinoma, and Barrett's epithelium. Gastroenterology *141*, 1762–1772.
29. Fujii, M., Shimokawa, M., Date, S., Takano, A., Matano, M., Nanki, K., Ohta, Y., Toshimitsu, K., Nakazato, Y., Kawasaki, K., et al. (2016). A Colorectal Tumor Organoid Library Demonstrates Progressive Loss of Niche Factor Requirements during Tumorigenesis. Cell Stem Cell *18*, 827–838.
30. Chumduri, C., Gurumurthy, R.K., Berger, H., Dietrich, O., Kumar, N., Koster, S., Brinkmann, V., Hoffmann, K., Drabkina, M., Arampatzi, P., et al. (2021). Opposing Wnt signals regulate cervical squamocolumnar homeostasis and emergence of metaplasia. Nat. Cell Biol. *23*, 184–197.
31. Xu, Y., Luo, H., Hu, Q., and Zhu, H. (2021). Identification of Potential Driver Genes Based on Multi-Genomic Data in Cervical Cancer. Front. Genet. *12*, 598304.
32. Jia, Q., Wang, J., He, N., He, J., and Zhu, B. (2019). Titin mutation associated with responsiveness to checkpoint blockades in solid tumors. JCI Insight *4*, e127901.
33. The Cancer Genome Atlas Research Network, and al, ect (2017). Integrated genomic and molecular characterization of cervical cancer. Nature *543*, 378–384.
34. Berger, A.C., Korkut, A., Kanchi, R.S., Hegde, A.M., Lenoir, W., Liu, W., Liu, Y., Fan, H., Shen, H., Ravikumar, V., et al. (2018). A Comprehensive Pan-Cancer Molecular Study of Gynecologic and Breast Cancers. Cancer Cell *33*, 690–705.e9. https://doi.org/10.1016/j.ccell.2018.03.014.
35. Abu-Rustum, N.R., Yashar, C.M., Bean, S., Bradley, K., Campos, S.M., Chon, H.S., Chu, C., Cohn, D., Crispens, M.A., Damast, S., et al. (2020). NCCN Guidelines Insights: Cervical Cancer, Version 1.2020. J. Natl. Compr. Canc. Netw. *18*, 660–666.
36. Meléndez, B., Van Campenhout, C., Rorive, S., Remmelink, M., Salmon, I., and D'Haene, N. (2018). Methods of measurement for tumor mutational burden in tumor tissue. Transl. Lung Cancer Res. *7*, 661–667.
37. Verdegaal, E.M.E., de Miranda, N.F.C.C., Visser, M., Harryvan, T., van Buuren, M.M., Andersen, R.S., Hadrup, S.R., van der Minne, C.E., Schotte, R., Spits, H., et al. (2016). Neoantigen landscape dynamics during human melanoma-T cell interactions. Nature *536*, 91–95.
38. Cattaneo, C.M., Dijkstra, K.K., Fanchi, L.F., Kelderman, S., Kaing, S., van Rooij, N., van den Brink, S., Schumacher, T.N., and Voest, E.E. (2020). Tumor organoid-T-cell coculture systems. Nat. Protoc. *15*, 15–39.
39. Carvalho, N.d.O., del Castillo, D.M., Perone, C., Januário, J.N., Melo, V.H.d., and Brasileiro Filho, G. (2010). Comparison of HPV genotyping by type-specific PCR and sequencing. Mem. Inst. Oswaldo Cruz *105*, 73–78.
40. Li, H. (2013). Aligning Sequence Reads, Clone Sequences and Assembly Contigs with BWA-MEM. Preprint at arXiv. https://doi.org/10.48550/arXiv.1303.3997.
41. Freed, D., Aldana, R., Weber, J.A., and Edwards, J.S. (2017). The Sentieon Genomics Tools – A Fast and Accurate Solution to Variant Calling from Next-Generation Sequence Data. Preprint at bioRxiv. https://doi.org/10.1101/115717.
42. Wang, K., Li, M., and Hakonarson, H. (2010). ANNOVAR: functional annotation of genetic variants from high-throughput sequencing data. Nucleic Acids Res. *38*, e164.
43. Talevich, E., Shain, A.H., Botton, T., and Bastian, B.C. (2016). CNVkit: Genome-Wide Copy Number Detection and Visualization from Targeted DNA Sequencing. PLoS Comput. Biol. *12*, e1004873.
44. Ding, R.B., Chen, P., Rajendran, B.K., Lyu, X., Wang, H., Bao, J., Zeng, J., Hao, W., Sun, H., Wong, A.H.H., et al. (2021). Molecular landscape and subtype-specific therapeutic response of nasopharyngeal carcinoma revealed by integrative pharmacogenomics. Nat. Commun. *12*, 3046.
45. Chandler, B.C., Moubadder, L., Ritter, C.L., Liu, M., Cameron, M., Wilder-Romans, K., Zhang, A., Pesch, A.M., Michmerhuizen, A.R., Hirsh, N., et al. (2020). TTK inhibition radiosensitizes basal-like breast cancer through impaired homologous recombination. J. Clin. Invest. *130*, 958–973.

STAR★METHODS

KEY RESOURCES TABLE

REAGENT or RESOURCE	SOURCE	IDENTIFIER
Antibodies		
Mouse monoclonal anti- CEA	ZSGB-BIO	Cat# ZM-0062
Mouse monoclonal anti- P53	ZSGB-BIO	Cat#ZM-0408
Mouse monoclonal anti- CK5/6	ZSGB-BIO	Cat# ZM-0313
Rabbit monoclonal anti- P16	Affinity	Cat# AF0228-50
Rabbit monoclonal anti- KI67	Proteintech	Cat# 27309-1-AP; RRID: AB_2756525
Mouse monoclonal anti- P63	ZSGB-BIO	Cat#ZM-0406
mouse anti-human HLA-ABC	Biolegend	Cat# 311402; RRID: AB_314871
mouse anti-human HLA-DR/DP/DQ	Biolegend	Cat# 361702; RRID: AB_2563139
PerCP/Cy5.5 anti-human CD3	Biolegend	Cat# 317335; RRID: AB_2561627
FITC anti-human CD4	Biolegend	Cat# 317407; RRID: AB_571950
Pacific Blue anti-human CD8	Biolegend	Cat# 344717; RRID: AB_10551616
APC anti-human CD137(4-1BB)	Biolegend	Cat# 309809; RRID: AB_830671
PE anti-human CD107a(LAMP-1)	Biolegend	Cat#328607; RRID: AB_1186062
Chemicals, peptides, and recombinant proteins		
Advanced DMEM/F-12	Thermo Fisher Scientific	Cat# 12634-010
GlutaMAX	Life Technologies	Cat# 35050061
HEPES	Life Technologies	Cat# 15630-056
Penicillin/streptomycin	Thermo Fisher Scientific	Cat# 15140-122
amphotericin B	Solarbio	Cat#A8250
collagenase II	Solarbio	Cat#C8150
Y-27632	Stemcell	Cat# 72304
growth factor-reduced Matrigel	CORNING	Cat# 356231
B27 supplement	Life Technologies	Cat# 17504-044
N2 supplement	Life Technologies	Cat# 17502048
N-acetyl-L-cysteine	Sigma-Aldrich	Cat# A9165
nicotinamide	Sigma-Aldrich	Cat# N0636
Noggin	PeproTech	Cat# 120-10C
A83-01	Sigma-Aldrich	Cat#SML0788
human epidermal growth factor	PeproTech	Cat# AF-100-15
forskolin	Abmole	Cat# M2191
hydrocortisone	Stemcell	Cat# 07925
R-spondin 1	PeproTech	Cat# 120-38
CHIR 99021	Sigma-Aldrich	Cat# SML1046
human fibroblast growth factor 2	PeproTech	Cat# 100-18B
human fibroblast growth factor 7	PeproTech	Cat# 100-19
prostaglandin E2	Cayman	Cat# 14010-1
TrypLE	GIBCO	Cat# 12604021
X-Vivo 15 Lymphocyte medium	Lonza	Cat# 04-418Q
IL-2	PeproTech	Cat# 200-02
Cell Recovery Solution	CORNING	Cat# 354253

(*Continued on next page*)

Continued

REAGENT or RESOURCE	SOURCE	IDENTIFIER
Critical commercial assays		
FastPure Cell/Tissue DNA Isolation Mini Kit	Vazyme	Cat# DC102-01
CellTiter-Glo 3-D Reagent	Promega	Cat# G9681
Cell-Trace Far Red	invitrogen	Cat# C34564
Caspase 3/7 probe	invitrogen	Cat# C10723
IFNγ ELISA kit	DAKEWE	Cat# 1110002
Software and algorithms		
R	S. Urbanek & H.-J. Bibiko	http://www.R-project.org

RESOURCE AVAILABILITY

Lead contact

Further information and requests for resources and reagents should be directed to and will be fulfilled by the lead contact, Shuzhong Yao (yaoshuzh@mail.sysu.edu.cn).

Materials availability

There are restrictions to the availability of cultured organoids due to limited quantity.

Data and code availability

- The gene mutation data have been deposited to the Supplemental table and are publicly available to as the date of publication.
- This paper does not report original code.
- Any additional information required to reanalyze the data reported in this paper is available from the lead contact upon request.

EXPERIMENTAL MODEL AND STUDY PARTICIPANT DETAILS

This study was conducted in accordance with the Regulations of the People's Republic of China on the Administration of Human Genetic Resources and was approved by the Ethics Committee of the First Affiliated Hospital of Sun Yat-sen University (Guangzhou, China). From January 2021 to December 2021, tissues, blood samples, and data were collected from cervical cancer patients who provided informed consent at the Department of Gynecology and Obstetrics of the First Affiliated Hospital of Sun Yat-sen University. The clinicopathological features of patients were shown in Table 1.

METHOD DETAILS

Tissue procession

After being washed three to five times with normal saline, each obtained tissue was preserved in Advanced DMEM+/+/+/+ (Advanced DMEM/F12 from Life Technologies), supplemented with 1× GlutaMAX, penicillin-streptomycin, 0.5ug/ml amphotericin B, and 10 mmol/L HEPES. Upon arrival, the tissues were cut into pieces measuring 3-5mm3, and small pieces were randomly divided for DNA isolation, pathological analysis, organoid derivation, and *ex vivo* expansion of tumor-infiltrating lymphocytes (TILs). (Figure 1A).

Small pieces for organoid culture were digested in 0.5 mg/ml collagenase II in Advanced DMEM+/+/+/+ on an orbital shaker at 37°C and 120 rpm. To prevent anoikis, an RHO/ROCK pathway inhibitor Y-27632 was added to the digestion media at a concentration of 10μM. After 1-2 hours of digestion, the suspension was filtered through a 100μm filter, and large pieces were collected to undergo further mechanical enzymatic processing. The resulting suspension was then centrifuged at 4°C and 1,200 rpm, and the cell pellet was washed twice with Advanced DMEM+/+/+/+ after red blood cell lysis using Beyotime reagent. The cell pellet was resuspended in ice-cold growth factor-reduced Matrigel, and droplets ranging from 3-40μL were plated on the bottom of pre-warmed CORNING's 24-well culture plates. The plates were inverted in a cell incubator for solidification of the Matrigel droplets for approximately 30 minutes before being covered with corresponding culture media as described below.

Organoids derived from cervical squamous carcinoma were cultured in Wnt-excluded medium, which was Advanced DMEM+/+/+ (Advanced DMEM/F12 supplemented with GlutaMAX and penicillin-streptomycin) supplemented with 1x B27 supplement, 1x N2 supplement, and 1 unit of an unspecified component. The medium also contained the following components: 25 millimoles of N-acetyl-L-cysteine, 10 millimoles of nicotinamide, 100 nanograms per milliliter of Noggin, 500 nanomoles of A83-01, 10 nanograms per milliliter of human epidermal growth factor, 100 nanograms per milliliter of human fibroblast growth factor 10, 10 micromoles of forskolin, and 500 nanograms per milliliter of hydrocortisone. Organoids derived from cervical adenocarcinoma were cultured in a Wnt-included medium containing B27, N-acetyl-L-cysteine, nicotinamide, A83-01, 200 nanograms per milliliter of R-spondin 1 and 40 nanograms per milliliter of Noggin.

This medium also included 3 micromoles of CHIR 99021, 50 nanograms per milliliter of human epidermal growth factor, 5 nanograms per milliliter of human fibroblast growth factor 2, 25 nanograms per milliliter of human fibroblast growth factor 7, 10 nanograms per milliliter of human fibroblast growth factor 10, and 1 micromole of prostaglandin E2 . Organoids were observed every 2-3 days while changing the culture medium. The organoids were passaged every 1-3 weeks using TrypLE, with a splitting ratio ranging from 1:2 to 1:10.

TILs *ex vivo* expansion

The TILs were expanded *ex vivo* as explained in.[37] Small pieces of tumor tissue were placed in the wells of 24-well plates. Then, X-Vivo 15 Lymphocyte medium with 6000 IU/mL IL-2 was added. The TILs were cultured in a cell incubator for 2 weeks before their expansion.

H&E staining and IHC

Gently dissolve organoids from Matrigel using a Cell Recovery Solution. Then, fix the organoids and paired tissues in 4% paraformaldehyde. After dehydration and paraffin embedding, sections are subjected to H&E staining and IHC. The antibodies used for IHC include CEA, P53, CK5/6, P16, KI67, and P63. After staining, the sections are analyzed by a professional pathologist.

DNA extraction and HPV detection

Following the protocol of the FastPure Cell/Tissue DNA Isolation Mini Kit , we extracted DNA from tissue, blood samples, and organoids. The quality and concentration of the DNA were assessed using a NanoDrop spectrophotometer. HPV infection was detected using real-time fluorescence quantitative PCR.[39] The positive infection standard was Ct <30, and the melting peak matched the standard peak. The high-risk HPV primers used were as follows.

HPV 16 forward: CAGACGACTATCCAGCGACC,
HPV 16 reverse: GCAGTGAGGATTGGAGCACT,
HPV 18 forward: CTGCTACACGACCTGGACAC,
HPV 18 reverse: CACCGAGAAGTGGGTTGACA,
HPV 33 forward: GCAACAACACGTACCAGCAA,
HPV 33 reverse: CAGGGCCAGACATAACAGGA.
Agarose gel electrophoresis was used to visualize HPV infection in the tissues and organoids.

Genomic analysis and TMB

Following DNA library preparation using the SureselectXT reagent kit (Agilent), WES (2×150 bp) was performed on an Agilent SureSelect V6 and Novaseq 6000 to an average coverage of 235× (Mingma Technologies, Shanghai, China). Briefly, after quality control, the Maximal Exact Matched algorithm in BWA (V0.7.17) was used to map the reads to the reference genome GRCh37.[40] Corresponding to the blood sample, somatic mutations and indels of the tumor and paired organoids were independently analyzed. Mutation detection and genotyping were performed using Sentieon (202010.01).[41] Annovar (Date 20180416) was used to annotate the identified mutation loci.[42] Used about 200bp bin size was used to analyze the copy number of each sample using CNVkit (0.9.9).[43] Tumor mutation burden (TMB) refers to the number of somatic mutations in the tumor genome after germline mutations are removed. Defined as the total number of somatic gene coding errors, base substitutions, gene insertions, or deletions detected per megabase. We calculated the tumor mutational burden for each sample based on the MAF file using the TMB function in R package maftools with default parameters: size = 50, log Scale = TRUE.[36]

Ex vivo organoids radiation and chemosensitization treatment

Tumor organoids in good condition were collected, passaged, and reseeded in 48-well plates at a density of 10,000 cells in 30ul Matrigel drops. For the radiosensitivity test, each group of organoids was exposed to X-rays (160 kV, 25mA, 0.3 mmCu filters, RS2000) when reached an average size (100 um in diameter). 2 weeks after radiation, CellTiter-Glo 3-D Reagent was used to measure the ATP levels in each group. According to the manufacturer's instructions, a multilabel analyzer (Infinite F500, TECAN) was used to measure luminescence.[44] For the result analysis, organoid viability was determined using the 0 Gy dose group as a reference (100%).

To determine the appropriate concentration of combined chemical drugs, the viability of the organoids was initially assessed using various concentrations of cisplatin (Figure S4). For *ex vivo* radiation and chemosensitization Treatment, organoids were treated with either radiation alone or radiation combined with 5uM cisplatin, and radiation treatment was administered before cisplatin addition. Organoid viability were measured.[44] To demonstrate whether CRT has a synergistic effect, three dose-response curves were measured, including the radiation treatment alone curve, combinational treatment curve, and theoretical additive effect curve. The predictive additive killing effect was calculated as $E_{Total} = E_1 + E_2 - E_1 \times E_2$ (where E_1 is the inhibitory effect of cisplatin at a concentration of 5μM and E_2 is the inhibitory effect of dose X at defined concentrations).[44] When the dose-response curve of combinational treatment was lower than the additive effect curve, it was classified as effective chemosensitization.

Organoids killing assay

After expansion, the TILs and autologous tumor organoids were collected, and their co-culture system was established.[38] Briefly, Before co-cultured, incubated plate with 5 μg/mL anti-CD28 antibody for 24h at 4°C. Gently dissolved autologous tumor organoids from Matrigel were

stained with Cell-Trace Far Red and Caspase 3/7 probe (Invitrogen) for organoid visualization and cell apoptosis analysis. Using MHC-blocked organoids co-cultured with paired TILs as controls, 150 μg/mL mouse anti-human HLA-ABC and 30 μg/mL mouse anti-human HLA-DR/DP/DQ, were incubated with dissociated organoids for 30 min at 37°C to block MHC-I and MHC-II. the dissociated part of organoids was into single cells and TILs were collected for cell counting to satisfy the effector: target (E: T) ratio= 10:1. After 72 h of co-culture, fluorescence micro-images were obtained to visualize organoid apoptosis. The cells and supernatant were collected for subsequent analysis. IFN-γ levels in the supernatant were examined using ELISA.

Flow cytometry

After the killing assay, pre-stained (Cell-Trace Far Red and Caspase 3/7 probe) tumor organoids were dissociated into single cells for quantification of apoptosis by flow cytometry. To analyze patient-specific TILs activation, TILs were collected, washed in FACS buffer, and stained with PerCP/Cy5.5 anti-human CD3, FITC anti-human CD4, Pacific Blue anti-human CD8, APC anti-human CD137, and PE anti-human CD107a for 30 min. The cells were washed twice before flow cytometric recording.

Organoid xenograft and In vivo PDOX radiotherapy

Ethical approval for the *in vivo* study was obtained from the Institutional Animal Care and Use Committee (IACUC) of Sun Yat-sen University. One week after passaging, organoids were recovered from Matrigel and resuspended at a density of 20,000 cells per 100ul in a 30% Matrigel/culture medium. Organoid suspensions were subcutaneously injected into 6-10 weeks-old female NCG(NOD/ShiLtJGpt-Prkdcem26Cd52Il2rgem26Cd22/Gpt) mice. The tumor size was measured weekly using a digital caliper after the mass was palpable. Tumor volume= (length ×width2) × π/6. Nine weeks after the injection, the mice were sacrificed, and the tumors were excised for further histological analysis.

For *in vivo* PDOX radiotherapy, after tumors grew to approximately 100mm3, radiation treatment was administered in six doses of 2 Gy.[45] Nine weeks after the injection, the mice were sacrificed, and the tumors were excised for further histological analysis.

QUANTIFICATION AND STATISTICAL ANALYSIS

Statistical methods are outlined in the respective figure legends. R version 4.0 and GraphPad Prism version 8 were used for statistical analysis. Student's t-test and ANOVA variance were used to compare continuous data between the groups. The chi-squared test was used to analyze the correlation between tumor organoids and clinicopathological parameters. Each experiment was performed in triplicate. $P < 0.05$ was considered statistically significant.